Published in final edited form as:
Angew Chem Int Ed Engl. 2008 ; 47(35): 6707–6711. doi:10.1002/anie.200802223.

Functional Analysis of an Aspartate-Based Epoxidation Catalyst with Amide-to-Alkene Peptidomimetic Catalyst Analogues**

Charles E. Jakobsche, **Gorka Peris**, and **Scott J. Miller***
Department of Chemistry Yale University 225 Prospect Street New Haven, CT 06520-4900 USA

Keywords

epoxidation; peptide; asymmetric catalysis; olefin isostere; fluorine; peptidomimetic

The biosynthesis of natural products that contain epoxides represents a powerful stimulus for the study of "epoxidase" enzymes.[i] Likewise, these processes have inspired a generation of science focused on small molecule catalysts that mediate selective epoxidations through a variety of mechanisms.[ii] With respect to the naturally occurring epoxidases, the mechanistic basis of *O*-atom transfer is often associated with the chemistry of either flavinoid cofactors, P450 enzymes containing a heme group, or chloroperoxidases that lead to stepwise ring formation.[iii] In thinking about the known biosynthetic apparatus for epoxide formation, we became curious about an alternative mode for *O*-atom transfer – one based on functional groups available in proteins, but perhaps not well-documented in the biosynthesis of epoxides. In particular, we speculated and recently showed that aspartic-acid-containing peptides (e.g., **1**; Figure 1a) might shuttle between the side-chain carboxylic acid and the corresponding peracid (e.g., **2**) creating a catalytic cycle competent for asymmetric epoxidation with turnover of the aspartate-derived catalyst. Such an approach is orthogonal to the Julia-Colonna epoxidation, a complementary peptide-based epoxidation based on a nucleophilic mechanism.[iv] Indeed, as shown in Figure 1b, this new electrophilic epoxidation catalytic cycle mediates the asymmetric epoxidation of substrates like **3** to give products like **4** with up to 92% ee.[v]

Mechanistic questions abound in this catalytic system. To date, we have identified a number of relevant aspects. For example, we observed off-catalytic cycle intermediates, including catalytically inactive diacyl peroxides (**6**).[vi] We also showed that these off-cycle intermediates could be reinserted into the productive pathway through the action of nucleophiles such as DMAP or DMAP-*N*-oxide (**7**). On the other hand, the basis of stereochemical information transfer was not immediately clear. Indeed, the high precision delineation of the stereochemical mode of action of chiral catalysts is a critical frontier in the discipline of asymmetric catalysis, whether the catalysts are enzymes or small molecules. With this back-drop, we began a detailed study of the mode of action for catalyst **5**.

The conversion of **3** to **4** was originally undertaken with the hypothesis that substrate-catalyst hydrogen bonding might contribute to transition state organization.[vii] Indeed, a substrate lacking obvious H-bonding capability (phenylcyclohexene) was found to undergo epoxidation with catalyst **5** with low enantioselectivity (~10% ee). Thus, we envisioned several potential loci for contacts between **3** and **5** (Figure 2a). Shown in blue is the site that

**We thank the NIH (National Institute of General Medical Sciences) and Merck Research Laboratories, each for partial support.

*Fax: (+1)-203-496-4900 scott.miller@yale.edu.

Supporting information for this article is available at http://www.angewandte.org or from the author.

represents possible Henbest-type interactions (e.g., ensembles **A** and **B**).[viii] Shown in red are other H-bonding sites that might contribute to the preferential formation of **4**. Of these, hand-held models suggested that **C** is consistent with the formation of the major enantiomer. Nevertheless, we sought to interrogate each potential binding site to identify the site(s) of interaction.

To evaluate the importance of the NHBoc functionality, we synthesized catalyst analogue **8**, in which the NHBoc group is replaced with a methyl group.[ix] As shown by X-ray crystallography (Figure 3), analogue **8** adopts the expected Type-II β-turn in the solid state.[x,xi] Notably, when catalyst **8** is evaluated in the asymmetric epoxidation of **3** under a common set of conditions (23 °C; $PhCH_3$, 12 h),[xii] product **4** is produced with 88% ee, which is analogous to that observed with original catalyst **5**. The fact that peptides **5** and **8** are both selective catalysts suggests that they likely exhibit similar three-dimensional structures. In this vein, the data suggests that the NHBoc group is not involved in an important H-bonding interaction with substrate.

For the functional evaluation of the Pro-DVal amide, we turned to the application of alkene isosteric replacements of the amide bond.[xiii] We have previously used this strategy in the mechanistic dissection of peptide-based asymmetric acylation catalysts.[xiv] We therefore sought to synthesize and study catalyst **9** (Figure 4a). Peptide **9** was prepared in five steps from known compound **10**.[xv,xvi]

From the functional perspective, catalyst **9** affords a result that suggests that the Pro-DVal amide could well be involved in a catalyst–substrate H-bond in the transition state. As shown in Figure 4b, the conversion of **3** to **4** occurs with a much-reduced 16% ee under catalysis by peptide **9**. Notably, our observations suggest that self-epoxidation of catalyst **9** is significantly slower than epoxidation of substrate **3** under these conditions.[xvii]

Perhaps of great significance, however, is the observation that peptidomimetic catalyst **9** exhibits conformational properties that are surprisingly different from catalyst **5**. Whereas catalyst **5** appears as a single conformation in solution by ^{1}H NMR (400 MHz), consistent with the β-turn observed in the X-ray structure of **8**, catalyst **9** appears as a heterogeneous 3.5:1 mixture of two distinct catalyst conformations (Figure 5, below). Notably, the signals coalesce when the NMR sample is heated to 100 °C (DMSO-d_6 solvent). Nevertheless, the lack of good homology between the room temperature conformational profiles of catalysts **5** and **9** warranted additional experiments to ascertain the functional role of the Pro-DVal amide in catalyst **5**.

Whereas dipeptide alkene isosteres have been found to be good steric mimics of amide bonds in peptides and proteins,[xviii] it is also well-recognized that they provide a poor mimic of other properties intrinsic to amides. In order to recapture amide-like character in an olefinic mimic, dipeptide fluoro-olefin isosteres have been introduced.[xix] In this context, it is also increasingly appreciated that the structural features that cause peptides to adopt secondary structures (including β-turns) are complex. In addition to hydrogen bonding,[xx] allylic strain about the Pro-DVal amide,[xxi] dipole neutralization of the Pro-DVal carbonyl,[xxii] and n-to-π^* donation[xxiii] from the Xaa-Pro carbonyl lone pair to the Pro-Yaa carbonyl may each contribute to the β-turn's stability.

Stimulated by these ideas, we undertook a synthesis of catalyst analogue **11**. Our hypothesis was that the fluoro-alkene moiety would be a better mimic of the local properties contributing to faithful β-turn nucleation, and that this catalyst would therefore be a better probe of catalyst **5**.

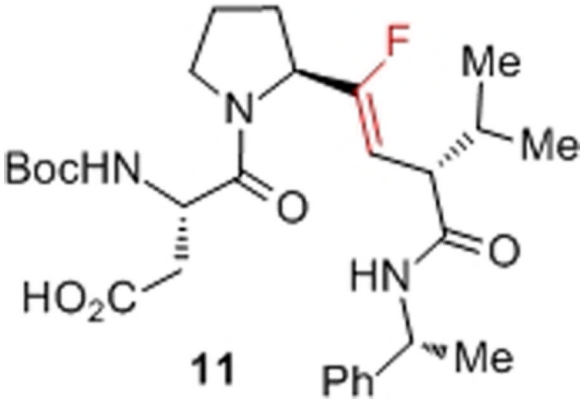

Scheme 1 shows the synthesis of fluoroalkene isostere **11**.[xxiv] The catalyst was prepared in twenty-one steps and 2% overall yield from phenylalanine (sixteen steps from compound **12**).[9,xxv] The stereochemistry of enoate **16** was set by a two-step olefination procedure. The stereogenic center in sulfinamide **20** was introduced using an auxiliary-controlled reductive amination.[xxvi] Oxidation of alcohol **22** and coupling to amine **23** gave catalyst **11**.[xxvii]

Indeed, fluoroalkene **11** proves to be conformationally more robust than alkene-isostere catalyst **9**. Whereas the ^{1}H NMR spectra for catalyst **9** reveal a 3.5:1 conformational mixture (23 °C), fluoro-alkene catalyst **11** exhibits an approximately 10:1 mixture of conformations at the same temperature (Figure 5). Once again, coalescence of the spectrum is observed when the sample is examined by ^{1}H NMR at 100 °C (DMSO-d_6).

Further ^{1}H NMR data (^{1}H-^{1}H NOESY) support the conformational analogies between peptide **5** and the major conformers of both **9** and **11** (Figure 6). These data suggest that the original peptide and the major conformations of the isosteres adopt β-turn structures similar to that exhibited in the crystal structure of peptide **8** (see Figure 3 above).

The actual asymmetric epoxidation reactions catalyzed by **11** offer intriguing results, delivering the product with 52% ee – intermediate between the selectivity afforded by catalysts **5** (81% ee) and **9** (16 % ee) under a common set of conditions.

The intermediate selectivity observed with fluoroalkene isosteric catalyst **11** allows for a number of interpretations. One is that indeed, transition state **C** (Figure 2, above) may be the dominant pathway leading to the preferential formation of the major enantiomer in the conversion of **3** to **4**. The near eradication of enantioselectivity with catalyst **9** (16% ee) may signal the loss of operation of the dominant pathway, revealing a base level of enantioselectivity through simple “shape-selectivity” associated with the catalyst. The appearance of partially recovered enantioselectivity with catalyst **11** (52% ee; *cf.* 81% ee with **5**), might then be explained by a weaker, but still significant H-bonding interaction in the transition state involving catalyst **11**. The energetics of C=O···H-N hydrogen bonds versus C–F···H-N have been discussed in the literature, with some debate. Evidence against,[xxviii] and in favor of such interactions has been described.[xxix] In the present case, the structure-selectivity-relationship revealed by catalysts **5**, **9** and **11** may suggest that a continuum exists with these catalysts (Figure 8) that is consistent with a moderate, but attractive C–F···H-N interaction in the dominant transition state.

Finally, analysis of catalysts with olefinic replacements of the C-terminal amide is not straightforward due to the inevitable eradication of the β-turn structure that such a replacement entails. Nevertheless, catalyst **24**, lacking the C-terminal amide, leads to poor selectivity (16% ee; Figure 9), suggesting an important functional role for this residue. Yet,

the lack of conformational analogy between **5**/**9**/**11** and **24** complicates the analysis, in that the role of the C-terminal amide may be purely structural, providing functionality for the signature β-turn H-bonding motif.

Taken together, the experimental results highlight structure-selectivity relationships for a new class of epoxidation catalysts. Through the application of fluorine-substituted alkene isosteres for the mechanistic interrogation of peptide-based catalysts, we have gained several important insights. First, through a comparative study of amide-alkene-fluoroalkene series of catalysts, we have identified unambiguously a hot-spot of correlation between catalyst structure and performance. Moreover, we have shown that such a series may also highlight important conformational features that regulate catalyst conformation, and ultimately function. The detailed interrogation of structure-function relationships is a critical step for increasing our understanding of asymmetric catalysis. Mechanistic studies of peptide-based systems may also help to elevate our appreciation of analogies between synthetic catalysts and enzymes, an activity at the heart of biomimetic science.[xxx]

Supplementary Material

Refer to Web version on PubMed Central for supplementary material.

References

[i]. Ding Y, Seufert WH, Beck Q, Sherman DH. J. Am. Chem. Soc. 2008; 130:5492–5498. [PubMed: 18366166]

[ii]. a) Xia Q-H, Ge H-Q, Ye C-P, Liu Z-M, Su K-X. Chem. Rev. 2005; 105:1603–1662. [PubMed: 15884785] b) Johnson, RA.; Sharpless, KB. Comprehensive Organic Synthesis. Trost, BM., editor. Vol. Vol. 7. Pergamon; New York: 1991. p. 389c) Jacobsen, EN.; Wu, MH. Comprehensive Asymmetric Catalysis II. Jacobsen, EN.; Pfaltz, A.; Yamamoto, H., editors. Springer-Verlag; Berlin: 1999. p. 649d) Denmark SE, Wu ZC. Synlett. 1999:847–859.e) Yang D. Acc. Chem. Res. 2004; 37:497–505. [PubMed: 15311948] f) Shi Y, Y. Acc. Chem. Res. 2004; 37:488–496. [PubMed: 15311947] g) Aggarwal VK, Winn CL. Acc. Chem. Res. 2004; 37:611–620. [PubMed: 15311960] h) Lee S, Macmillan DWC. Tetrahedron. 2006; 62:11413–11424.i) Wang X, Reisinger CM, List B. J. Am. Chem. Soc. 2008; 130:6070–6071. [PubMed: 18422314] See also,

[iii]. Grüschow, S.; Sherman, DH. Aziridines and Epoxides in Organic Synthesis. Yudin, AK., editor. Wiley-VCH; Weinheim: 2006. p. 349

[iv]. a) Kelly DR, Roberts SM. Biopolymers. 2006; 84:74–89. [PubMed: 16167327] b) Berkessel A, Koch B, Toniolo C, Rainaldi M, Broxterman QB, Kaptein B. Biopolymers. 2006; 84:90–96. [PubMed: 16283656]

[v]. a) Peris G, Jakobsche CE, Miller SJ. J. Am. Chem. Soc. 2007; 129:8710–8711. [PubMed: 17592849] b) Berkessel A. Angew. Chem. Int. Ed. 2008; 47:3677–3679.

[vi]. a) Jain RP, Vederas JC. Org. Lett. 2003; 5:4669–4672. [PubMed: 14627411] b) Rebek J, McCready R, Wolf S, Mossman A. J. Org. Chem. 1979; 44:1485–1493.c) Greene FD, Kazan J. J. Org. Chem. 1963; 28:2168–2171.d) Spantulescu MD, Jain RP, Derksen DJ, Vederas JC. Org. Lett. 2003; 5:2963–2965. [PubMed: 12889919]

[vii]. Doyle AG, Jacobsen EN. Chem. Rev. 2007; 107:5713–5743. [PubMed: 18072808]

[viii]. a) Henbest HB, Wilson RAL. Chem. Ind. 1956; 26:659.b) Kocovsky P, Stary I. J. Org. Chem. 1990; 55:3236–3243.c) Hoveyda AH, Evans DA, Fu GC. Chem. Rev. 1993; 93:1307–1370.

[ix]. The details of the synthesis and characterization data may be found in the electronic Supporting Material.

[x]. a) Rose GD, Gierasch LM, Smith JA. Adv. Protein Chem. 1985; 37:1–109. [PubMed: 2865874] b) Haque TS, Little JC, Gellman SH. J. Am. Chem. Soc. 1996; 118:6975–6985.

[xi]. A colorless block crystal (0.25 × 0.20 × 0.20 mm^3) was mounted with epoxy cement on the tip of a fine glass fiber. All measurements were made on a Bruker Nonius Kappa CCD diffractometer

with graphite monochromated Mo-Kα radiation. The data were corrected for Lorentz and polarization effects. The data frames were processed and scaled using the DENZO software package. The structure was solved by direct methods and expanded using Fourier techniques. The non-hydrogen atoms were refined anisotropically and hydrogen atoms were treated as idealized contributions. $C_{23}H_{33}N_3O_5{\cdot}CH_2Cl_2 = C_{24}H_{35}Cl_2N_3O_5$, $M_r = 516.45$, crystal system = orthorhombic, space group = $P2_12_12_1$ (#19), unit cell: a = 9.0028(18) Å, b = 11.376(2) Å, c = 26.325(5) Å, α = 90°, β = 90°, γ = 90°, V = 2696.1(9) $Å^3$, Z = 4, $\rho_{calculated} = 1.272$ g/cm^3, μ = 2.78cm^{-1}, source: Mo-Kα radiation = 0.71073 Å, collected at 173(2) K, 2 $\theta_{max} = 57.90°$, 6950 independent reflections, $R_{int} = 0.000$ Friedel pairs not merged, R = 0.0473, $R_w = 0.0963$, residual electron density = 0.331 and 0.438 eA^{-3}, Cambridge Crystallographic Data Center, #687520.

[xii]. See Supporting Material for details.

[xiii]. a) Gante J. Angew. Chem Int. Ed. Engl. 1994; 33:1699–1720.b) Gardner RR, Liang G-B, Gellman SH. J. Am. Chem. Soc. 1995; 117:3280–3281.c) Wipf P, Henninger TC, Geib SJ. J. Org. Chem. 1998; 63:6088–6089. [PubMed: 11672228]

[xiv]. Vasbinder MM, Jarvo ER, Miller SJ. Angew. Chem. Int. Ed. 2001; 113:2906–2909.

[xv]. Ibuka T, Taga T, Habashita H, Nakai K, Tamamura H, Fujii N. J. Org. Chem. 1993; 58:1207–1214.

[xvi]. Details may be found in the Supporting Material. X-ray data has been deposited, CCDC#687519.

[xvii]. Corey EJ, Niwa H, Falck JR. J. Am. Chem. Soc. 1979; 101:1586–1587.

[xviii]. Wipf P, Xiao J, Geib SJ. Adv. Synth. Catal. 2005; 347:1605–1613.

[xix]. a) Bartlett PA, Otake A. J. Org. Chem. 1995; 60:3107–3111.b) Couve-Bonnaire S, Cahard D, Pannecoucke X. Org. Biomol. Chem. 2007; 5:1151–1157. [PubMed: 17406709] c) Urban JJ, Tillman BG, Cronin WA. J. Phys. Chem. A. 2006; 110:11120–11129. [PubMed: 16986846]

[xx]. Baldwin RL. J. Biol. Chem. 2003; 278:17581–17588. [PubMed: 12582164]

[xxi]. a) Deslauriers R, Becker JM, Steinfeld AS, Naider F. Biopolymers. 1979; 18:523–538.b) McDonald DQ, Still WC. J. Org. Chem. 1996; 61:1385–1391.

[xxii]. a) Park C, Goddard WA. J. Phys. Chem. B. 2000; 104:7784–7789.b) Gallo EA, Gellman SH. J. Am. Chem. Soc. 1994; 116:11560–11561.

[xxiii]. Hodges JA, Raines RT. J. Am. Chem. Soc. 2005; 127:15923–15932. [PubMed: 16277536]

[xxiv]. Sano S, Kuroda Y, Saito K, Ose Y, Nagao Y. Tetrahedron. 2006:11881–11890.Our scheme is based on the work of Sano. See:

[xxv]. a) Watson RJ, Batty D, Baxter AD, Hannah DR, Owen DA, Montana GJ. Tetrahedron Lett. 2002; 43:683–685.b) Boger DL, Hong J. J. Am. Chem. Soc. 2001; 123:8515–8519. [PubMed: 11525659]

[xxvi]. Dutheuil G, Couve-Bonnaire S, Pannecoucke X. Angew. Chem. Int. Ed. 2007; 46:1290–1292.

[xxvii]. The relative stereochemical relationships were shown by X-ray analysis of the amino alcohol derived from 21. Details of the synthesis may be found in the Supporting Material. X-ray data has been deposited, CCDC#687521.

[xxviii]. a) Dunitz JD, Taylor R. Chem. Eur. J. 1997; 3:89–98.b) Wang X, Houk KN. Chem. Commun. 1998:2631–2632.

[xxix]. a) Barbarich TJ, Rithner CD, Miller SM, Anderson OP, Strauss SH. J. Am. Chem. Soc. 1999; 121:4280–4281.b) Bettinger HF. ChemPhysChem. 2005; 6:1169–1174. [PubMed: 15945048]

[xxx]. Knowles JR. Nature. 1991; 350:121–124. [PubMed: 2005961]

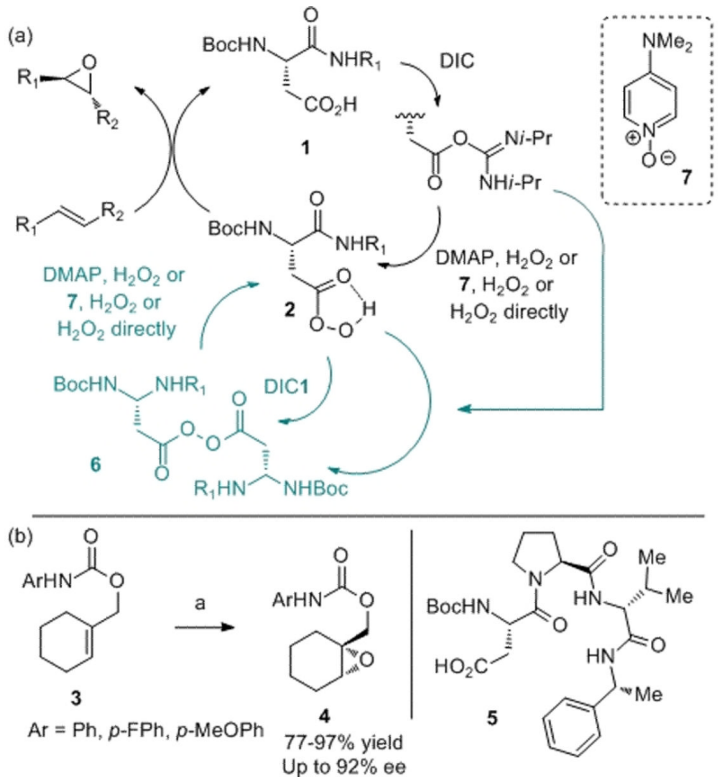

Figure 1.

(a) Previously reported catalytic cycle for epoxidation. **(b)** Asymmetric catalytic epoxidation with peptide **5**. Conditions: a) **5** (10 mol %), DIC (2.0 equiv), DMAP (10 mol %), H_2O_2 (30% aq, 2.5 equiv) or urea-H_2O_2 (2.5 equiv), DCM or toluene (1.0 M), −10 or 4 °C, 1–3 d.

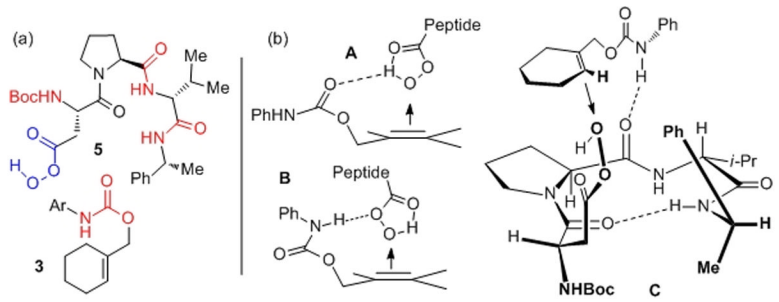

Figure 2.
(a) Possible catalyst-substrate H-bonding loci shown in color. (b) Representative transition state ensembles.

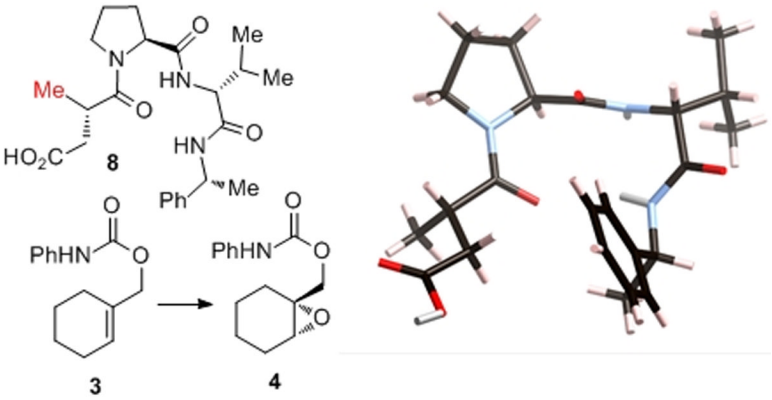

Catalyst	Ee (er)	Conversion
5[a]	92 (24:1)	76%
5[b]	81 (9.5:1)	63%
8[b]	88 (15.4:1)	26%

X-Ray Structure of **8**

[a] 4 °C, $PhCH_3$, urea/H_2O_2 complex, DIC, DMAP, 1.0 M; 33 h.

[b] 23 °C, $PhCH_3$, 30% H_2O_2, DCC, DMAP, 0.4 M; 12 h.

Figure 3.
Catalytic performance and X-ray analysis of peptide **8**.

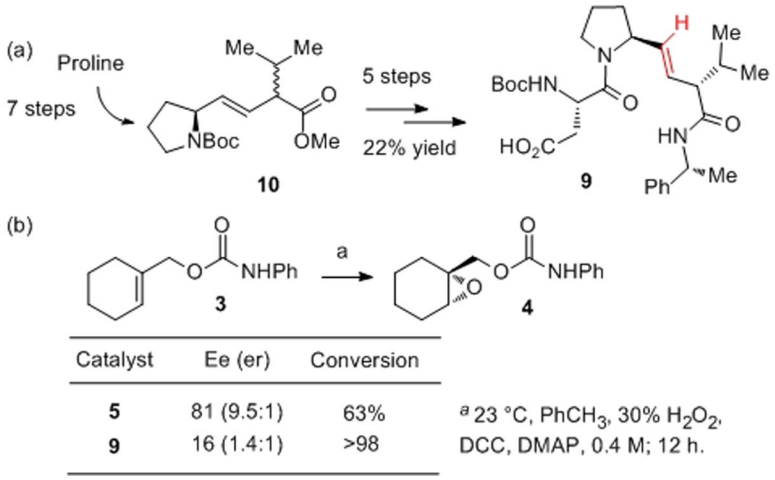

Catalyst	Ee (er)	Conversion
5	81 (9.5:1)	63%
9	16 (1.4:1)	>98

[a] 23 °C, $PhCH_3$, 30% H_2O_2, DCC, DMAP, 0.4 M; 12 h.

Figure 4.
(a) Synthesis and **(b)** Catalytic efficiency of **9**.

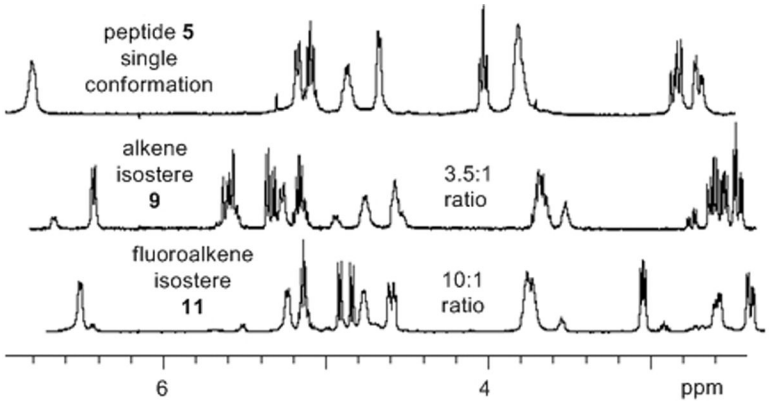

Figure 5.
Partial ^{1}H NMR spectra of catalysts **5**, **9** and **11**.

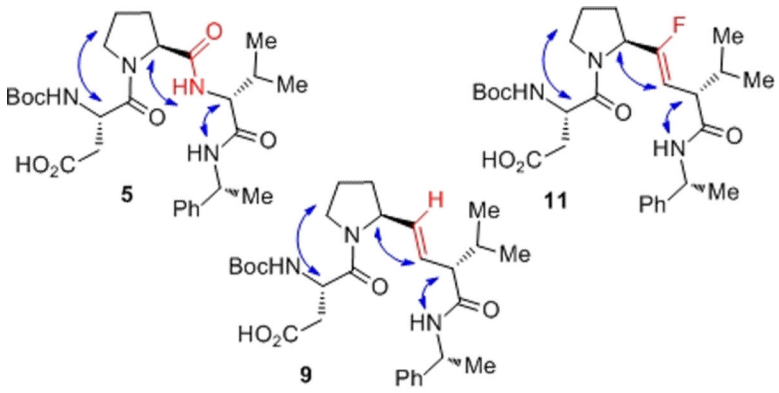

Figure 6.
Select NOE contacts from the major conformational isomers of peptide **5** and its isosteres **9** and **11**.

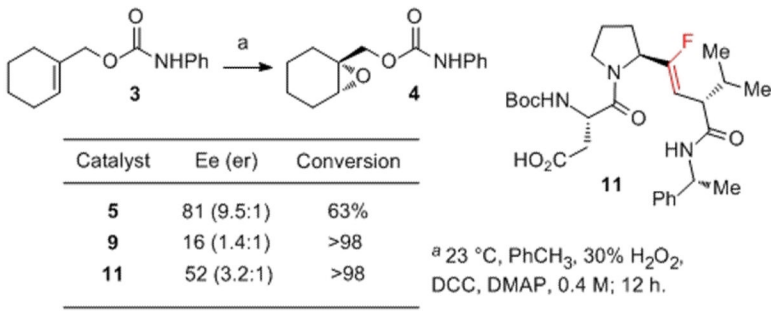

Catalyst	Ee (er)	Conversion
5	81 (9.5:1)	63%
9	16 (1.4:1)	>98
11	52 (3.2:1)	>98

[a] 23 °C, $PhCH_3$, 30% H_2O_2, DCC, DMAP, 0.4 M; 12 h.

Figure 7.
Catalytic epoxidation data with catalysts **5**, **9**, and **11**.

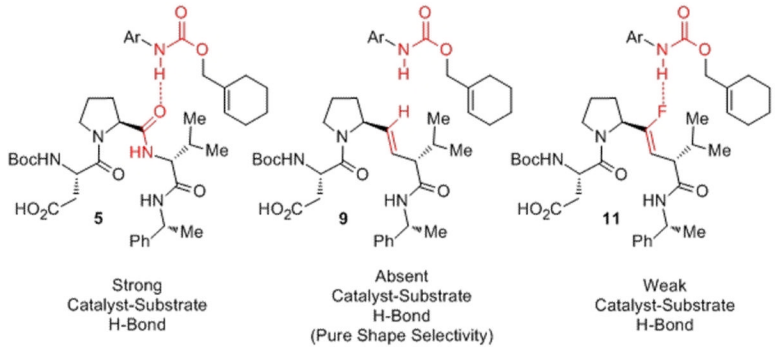

Figure 8.
A potential continuum between catalyst-substrate H-bonding interactions that track with observed enantioselectivity.

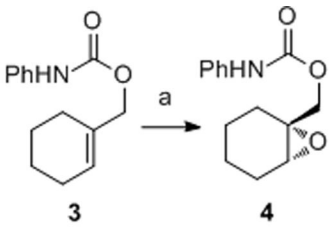

Catalyst	Ee (er)	Conversion
5	81 (9.5:1)	63%
24	16 (1.4:1)	>98%

[a] 23 °C, $PhCH_3$, 30% H_2O_2, DCC, DMAP, 0.4 M; 12 h.

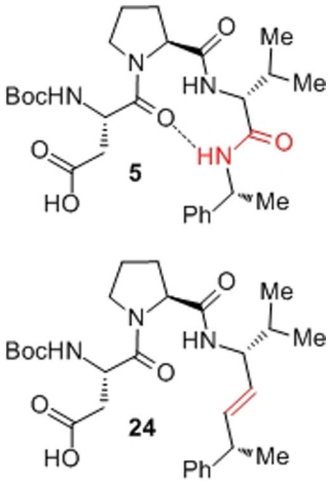

Figure 9.
Consequences of C-terminal amide replacements for ee.

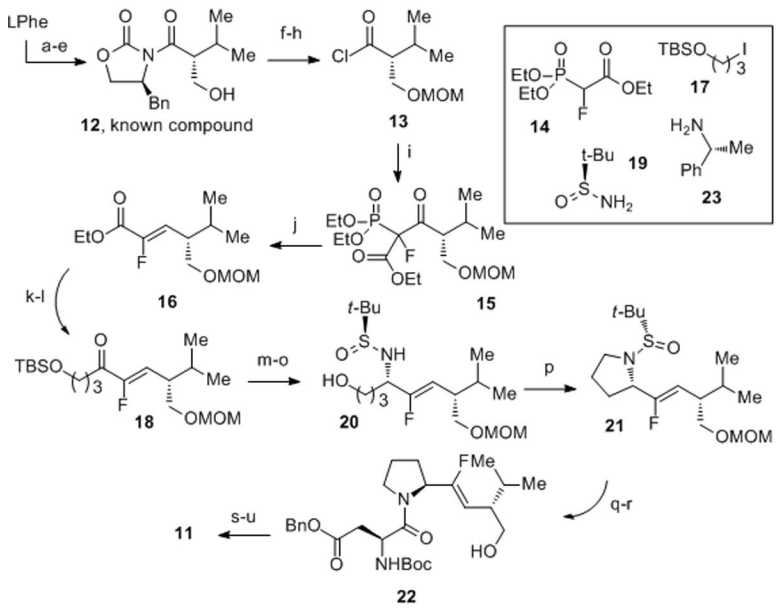

Scheme 1.

Synthesis of fluoroalkene isostere **11**: a–e) See Supporting Material; f) DiPEA, MOMCl, DCM, 0 °C, 2.5 h; g) LiOH, H_2O_2, THF, H_2O, 0° to 23 °C, 3 h; h) oxalyl chloride, DMF, ether, 23 °C, 15 min, 80% yield (3 steps); i) **14**, NaH, THF, 23 °C, 1 h, then **13**, −40 °C, 1 h, (5:1 dr, use mixture); j) $NaBH_4$, EtOH, −40 °C, 2.5 h, 69% (2 steps, >20:1 dr); k) MeNHOMeHCl, *i*-PrMgCl, THF, 0 °C, 1.5 h, 79%; l) **17**, ether, *t*-BuLi, −78° to 23 °C, 30 min, then Weinreb amide of **16**, −78 °C, 1 h, 59%; m) **19**, Ti(OEt)4, THF, reflux, 3 h; n) DiBAl-H, −78 °C, 3 h; o) TBAF, THF, 23 °C, 40 min, 95% (3 steps); p) DEAD, PPh_3, THF, 23 °C, 2 h, 80%; q) HCl/dioxane, MeOH, 23 °C, 1.5 h; r) Boc-Asp(OBn)-OH, EDC, HOBt, TEA, DCM, 23 °C, 14 h, 70% (2 steps); s) PDC, DMF, 23 °C, 6 h, 90%; t) **23**, EDC, HOBt, DCM, 23 °C, 14 h, 47%; u) LiOH, dioxane, water, 23 °C, 16 h, 89%.